

Diacylglycerols Activate Mitochondrial Cationic Channel(s) and Release Sequestered Ca²⁺

Christos Chinopoulos,¹ Anatoly A. Starkov,² Sergey Grigoriev,³ Laurent M. Dejean,³
Kathleen W. Kinnally,³ Xibao Liu,⁴ Indu S. Ambudkar,⁴ and Gary Fiskum^{1,5}

Received May 18, 2005; accepted May 31, 2005

Mitochondria contribute to cytosolic Ca²⁺ homeostasis through several uptake and release pathways. Here we report that 1,2-sn-diacylglycerols (DAGs) induce Ca²⁺ release from Ca²⁺-loaded mammalian mitochondria. Release is not mediated by the uniporter or the Na⁺/Ca²⁺ exchanger, nor is it attributed to putative catabolites. DAGs-induced Ca²⁺ efflux is biphasic. Initial release is rapid and transient, insensitive to permeability transition inhibitors, and not accompanied by mitochondrial swelling. Following initial rapid release of Ca²⁺ and relatively slow reuptake, a secondary progressive release of Ca²⁺ occurs, associated with swelling, and mitigated by permeability transition inhibitors. The initial peak of DAGs-induced Ca²⁺ efflux is abolished by La³⁺ (1 mM) and potentiated by protein kinase C inhibitors. Phorbol esters, 1,3-diacylglycerols and 1-monoacylglycerols do not induce mitochondrial Ca²⁺ efflux. Ca²⁺-loaded mitoplasts devoid of outer mitochondrial membrane also exhibit DAGs-induced Ca²⁺ release, indicating that this mechanism resides at the inner mitochondrial membrane. Patch clamping brain mitoplasts reveal DAGs-induced slightly cation-selective channel activity that is insensitive to bongkreikic acid and abolished by La³⁺. The presence of a second messenger-sensitive Ca²⁺ release mechanism in mitochondria could have an important impact on intracellular Ca²⁺ homeostasis.

KEY WORDS: Mitochondria; calcium; diacylglycerol; mitoplast; cation channel; permeability transition pore; protein kinase C; transient receptor potential; OAG.

INTRODUCTION

A plethora of cellular signaling cascades converge to the production of diacylglycerols (DAGs), leading to the activation of various target proteins regulating cellular processes of extraordinary diversity (Brose *et al.*, 2004). Depending on the identity of the stimulated receptor, dif-

ferent PLC isoforms are activated resulting in the immediate formation of DAG from inositol phospholipids, most rapidly from P1-4,5-bisphosphate (PIP₂). This DAG molecule disappears quickly; however, a second wave of DAG emerges with a relatively slow onset persisting for minutes or hours. This latent increase in DAG is partially attributed to the subsequent action of phospholipase D (PLD) on phosphatidylcholine (PC) to yield phosphatidate plus choline followed by phosphatidate phosphatase generating DAG and orthophosphate (Nishizuka, 1992,

¹ Department of Anesthesiology, University of Maryland, Baltimore, Maryland.

² Department of Neurology, Weill Medical College, Cornell University, New York, New York.

³ Division of Basic Sciences, New York University College of Dentistry, New York, New York.

⁴ Secretary Physiology Section, Gene Therapy and Therapeutics Branch, NIDCR, National Institutes of Health, Bethesda, Maryland.

⁵ To whom correspondence should be addressed at Department of Anesthesiology, University of Maryland School of Medicine, 685 West Baltimore Street, MSTF 5-34, Baltimore, Maryland 21201; e-mail: gfk001@umaryland.edu.

Abbreviations used: 1,2-DGs, 1,2-Diacylglycerols; 1,3-DGs, 1,3-Diacylglycerols; 2-MGs, 2-Monoacylglycerols; 1-MGs, 1-Monoacylglycerols; ALM, Alamethicin; BKA, Bongkreikic acid; Cys A, Cyclosporin A; PTP, Permeability Transition Pore; OAG, 1-oleoyl-acetyl-sn-glycerol; DOL, 1,2-Dioleoylglycerol (18:1); DDC, 1,2-Didecanoylglycerol (10:0); SAG, 1-stearoyl-2-arachidonoyl-sn-glycerol; DOG, 1,2-Dioctanoyl-sn-glycerol (8:0); HDAG, 1-O-Hexadecyl-2-arachidonoyl-sn-glycerol.

1995). An additional pathway contributing to this latency is substantiated by the slow degradation of DAG by DAG lipase; this DAG is produced from PC hydrolysis by phosphatidylcholine-specific phospholipase C and is a poor substrate for the fast-acting enzyme DAG kinase (Ford and Gross, 1990; Lee *et al.*, 1991). DAG kinase rapidly catabolizes DAG produced from phosphatidylinositol hydrolysis converting it to phosphatidate at the expense of ATP (Florin-Christensen *et al.*, 1992).

Downstream effects of DAGs are commonly attributed to activation of PKCs. There are, however, additional important targets of DAGs including protein kinase D (PKD), DAG kinases α , β , and γ , RasGRPs, chimaerins, Munc13s, and channels of the transient receptor potential (TRP) family, namely TRPC3, 6, and 7 (Brose *et al.*, 2004; Brose and Rosenmund, 2002; Hofmann *et al.*, 1999; Kazanietz, 2002; Okada *et al.*, 1999; Yang and Kazanietz, 2003).

Upon PIP₂ hydrolysis, DAGs are formed in a membrane-delimited manner both on the plasma membrane and on intracellular membranes (Irvine, 2002; Panagia *et al.*, 1991; Rebecchi and Pentylala, 2000), serving as hydrophobic anchors to recruit their targets to the membrane (Brose *et al.*, 2004). The other product, IP₃, diffuses in the cytosol to activate IP₃ receptors on the ER releasing Ca²⁺ to the cytoplasm followed by triggering of Ca²⁺ influx from the extracellular space (Mikoshiba and Hattori, 2000). Within the context of intracellular Ca²⁺ homeostasis, mechanisms and effectors downstream of the IP₃ signaling pathway received the vast majority of attention, culminating in a spark of interest on the so-called “store-operated Ca²⁺ entry” (SOCE) (Nilius, 2004; Penner and Fleig, 2004; Venkatachalam *et al.*, 2002). SOCE is a process whereby the depletion of intracellular Ca²⁺ stores (likely ER or SR) activates plasma membrane Ca²⁺ permeable channels (Putney, 1986). Members of the TRP family are candidates for SOCE; however, unequivocal evidence demonstrating that TRP channels account for this phenomenon is yet to be reported (Clapham, 2003; Nilius, 2004). Conversely, it has been shown that at least three members of the TRP family are activated by DAGs but not through PKC (Clapham *et al.*, 2003). These channels (TRPC3, 6, and 7) do not possess the DAG-binding C1 domain (Gudermann *et al.*, 2004), while TRPC3 plus two additional TRP channels, TRPC4 and TRPC5, are inhibited upon activation of PKC (Venkatachalam *et al.*, 2003).

Enzymes and macromolecules participating in the formation of DAGs have been reported to reside or translocate to mitochondria. PIP₂ is found in mitochondria (Watt *et al.*, 2002) and a brain-specific isomer may exist (Bothmer *et al.*, 1992); PLC δ is found in mitochon-

dria from liver (Knox *et al.*, 2004), yeast (Vaena de *et al.*, 2004), and kidney (Nishihira and Ishibashi, 1986). PLD and phosphatidate phosphatase exist in intestinal and myocardial mitochondria (Freeman and Mangiapane, 1989; Liscovitch *et al.*, 1999). The same is true for DAG targets: mitochondrial translocation of PKC δ is a critical proapoptotic event in cardiac responses following ischemia and reperfusion (Murriel *et al.*, 2004), as well as in phorbol ester-induced apoptosis in human myeloid leukemia cells (Majumder *et al.*, 2000) and keratinocytes (Li *et al.*, 1999). An alternative isoform PKC ϵ , confers beneficial effects upon translocation to mitochondria by inhibiting the permeability transition (Baines *et al.*, 2003), while others, such as PKC α , phosphorylate mitochondrial Bcl-2 suppressing apoptosis (Ruvolo *et al.*, 1998) or promote cardioprotection at least partially due to modulation of mitochondrial K⁺_{ATP} channels (Korge *et al.*, 2002; Sato *et al.*, 1998). With the exception of mitochondrial PKD (Storz *et al.*, 2000), the presence of other non-PKC targets of DAG has not been reported.

Based on the involvement of DAGs on multiple mitochondrial functions, we tested the hypothesis that this second messenger affects mitochondrial Ca²⁺ handling. We show that DAGs release Ca²⁺ from Ca²⁺-loaded mitochondria in conjunction with activation of novel channel(s) present on the inner mitochondrial membrane.

MATERIALS AND METHODS

Isolation of Mitochondria

All animal procedures were carried out according to the National Institutes of Health and the University of Maryland, Baltimore animal care and use committee guidelines. Adult male Sprague-Dawley rats and C57BL/6 mice were used. Nonsynaptic adult rat brain mitochondria were isolated on a Percoll gradient exactly as described previously (Chinopoulos *et al.*, 2003). Mouse heart, kidney, and liver mitochondria were prepared as described previously (Starkov and Fiskum, 2001). Mitochondria from sweet potato (*Ipomoea batatas*) were isolated as detailed previously (Chen and Lehninger, 1973).

Mitochondrial Ca²⁺ Uptake in Mammalian Mitochondria

Rat Brain

Mitochondrial or mitoplast-dependent (0.275 mg/mL) removal of medium Ca²⁺ was followed using

the impermeant pentapotassium salt of the ratiometric dye Fura 6F (Molecular Probes, Portland, OR, USA) as previously described in a KCl-based medium containing malate plus glutamate as respiratory substrates (Chinopoulos *et al.*, 2003). All experiments were performed at 37°C.

Rat Liver

The experiments were conducted as for rat brain mitochondria, with the exception that these mitochondria (0.5 mg/ml) were suspended in 250 mM sucrose, 20 mM Hepes, 2 mM KH_2PO_4 , 1 mM MgCl_2 , 5 mM succinate, 1 μM rotenone, 1 mg/ml bovine serum albumin (BSA, fatty acid-free), pH 7.2.

Mouse Heart and Kidney

These experiments were performed similar to the ones for rat brain, but at room temperature ($\sim 23^\circ\text{C}$), the fluorescent dye used was the hexapotassium salt of Calcium Green-5N (200 nM, $K_d = 4.3 \mu\text{M}$) (Rajdev and Reynolds, 1993), and the mitochondria (0.25 mg/ml) were suspended in 225 mM mannitol, 75 mM sucrose, 2 mM KH_2PO_4 , 5 mM HEPES, 0.2 mg/ml BSA (fatty acid-free) 5 mM glutamate, 5 mM malate, pH 7.4.

Mitochondrial Ca^{2+} Uptake in Sweet Potato Mitochondria

1 mg/ml of mitochondria was used; the experimental conditions were similar to those for mammalian mitochondria but performed at room temperature ($\sim 23^\circ\text{C}$) in 300 mM mannitol, 10 mM Hepes, 2 mM KH_2PO_4 , 10 mM succinate, 0.5 mM ADP, 2 mM ATP, plus 1 mg/ml BSA (fatty acid-free), pH 7.4.

Preparation of Mitoplasts From Rat Brain Mitochondria for Ca^{2+} Uptake Studies

Mitoplasts were prepared as described previously (Schnaitman *et al.*, 1967), with minor modifications: Upon isolation of mitochondria, protein determination was performed (Biuret); afterwards, 450–500 μL of 20 mg/ml mitochondria were suspended in 2.5 mL of buffer “A” containing 10 mM TRIS and 2 mM MgCl_2 , pH = 7.8 for 20 min in ice while shaking. Subsequently, 3 mL of 1.8 M Sucrose plus 2 mM MgCl_2 was added and left in ice while

shaking for an additional 20 min. Next, 12 mL of buffer A plus 45 μg of digitonin (>99% pure) was added to the suspension and left in ice while shaking for 15 min. At the end of this step, the suspension was diluted 5-fold with buffer “B” containing: 225 mM mannitol, 75 mM sucrose, 5 mM Hepes, 1 mM EGTA, 0.5 mg/ml BSA (fatty acid-free), pH = 7.4, and were centrifuged at 12,000 $\times g$ for 10 min. This centrifugation step was repeated once, and the resulting pellet was suspended in buffer B without EGTA. To evaluate the efficiency of the removal of the outer mitochondrial membranes, mitoplasts were tested for the presence of adenylate kinase, as described previously (Schmidt *et al.*, 1984); >95% of adenylate kinase activity was lost with this method. These mitoplasts retained a respiratory control ratio of 5 ± 1 over a period of 45 min (in the presence of externally added cyt *c*).

Preparation of Mitoplasts From Rat Brain Mitochondria for Patch Clamp Studies

Upon isolation of mitochondria, the organelles were suspended in a hypertonic buffer consisting of 460 mM Mannitol, 140 mM Sucrose, 10 mM HEPES, pH 7.4 for 10 min. Subsequently, they were subjected to 1500 psi with a French press (American Instruments Company, Silver Springs, MD, USA). The suspension was diluted with 2 volumes of 230 mM Mannitol, 70 mM Sucrose, 5 mM HEPES, pH 7.4. Mitoplasts were pelleted at 12,000 $\times g$ for 10 min and resuspended in 100 μL of the same buffer.

Oxygen Consumption

Mitochondrial respiration was recorded at 37°C with a Clark-type oxygen electrode (Hansatech, UK) as described previously (Chinopoulos *et al.*, 2003).

Mitochondrial Swelling

Swelling of isolated liver mitochondria was assessed by measuring light scatter at 540 nm (37°C) in a Beckman Coulter DU 7500 spectrophotometer (Fullerton, CA, USA) as detailed previously (Bernardi *et al.*, 1992).

Patch Clamp of Rat Brain Mitoplasts

Membrane patches were excised from rat brain mitoplasts after formation of a giga-seal (2–5 G Ω) using

glass electrodes made of borosilicate and resistances of 10–30 M Ω . The solution in the electrodes and bath was 150 mM KCl, 5 mM HEPES, pH 7.4. This buffer contained 10 μ M free Ca²⁺. Experiments were carried out at room temperature (~23°C). Voltage clamp was established with the inside-out excised configuration and currents were amplified using an Axopatch 200 amplifier (Union city, CA, USA). Current traces were sampled at 5 kHz with 2 kHz filtration and analyzed with WinEDR version v2.4.3 program (Strathclyde Electrophysiological Software courtesy of J. Dempster, Univ. of Strathclyde, UK). Ion selectivity was measured by a 1:5 gradient by perfusion of the bath with 30 mM KCl, 184 mM mannitol, 56 mM sucrose, 5 mM HEPES, pH 7.4.

Reagents

Standard laboratory chemicals were from Sigma. 2-APB (Sigma), CGP 37157 (Calbiochem), cyclosporin A (Sigma), bongkreikic acid (Calbiochem), alamethicin (Sigma), BSA (Sigma), Digitonin (Spectrum, New Brunswick, NJ, USA), PMA (Sigma), RHC 80267 (Calbiochem), DAG kinase inhibitor II (Sigma), all PKC inhibitors (Calbiochem, PKC inhibitor set), all 1,2-DGs and MGs were from Sigma or Biomol, all 1,3-DGs were from ICN Biomedicals (Aurora, OH, USA).

RESULTS

Release of Sequestered Ca²⁺ in Mammalian but Not Sweet Potato Mitochondria by OAG

Ca²⁺-loaded mitochondria from rat brain (Fig. 1(A)), mouse kidney (Fig. 1(B)), mouse heart (Fig. 1(C)), and rat liver (Fig. 1(E)) release Ca²⁺ upon exposure to the putative, cell-permeable diacylglycerol analogue, OAG. After the initial rapid release, Ca²⁺ was re-accumulated, followed by a secondary slow net release. In contrast to OAG, phorbol 12-myristate 13-acetate (PMA) failed to induce Ca²⁺ efflux (Fig. 1(A), trace *b*). Sweet potato mitochondria loaded with Ca²⁺ did not exhibit OAG-induced Ca²⁺ release (Fig. 1(D), trace *b*). Liver mitochondria pretreated with Cys A (Fig. 1(E), trace *b*) display an almost identical OAG-induced Ca²⁺ release and a moderate extent in the lag time until the spontaneous secondary efflux. Using identical conditions, swelling was not observed upon addition of OAG to Ca²⁺-loaded liver mitochondria (Fig. 1(G)); however, they exhibit spontaneous large amplitude swelling coincident with the secondary Ca²⁺ efflux in the absence (trace *a*) or presence (trace *b*) of Cys A. Cys A moderately extends the threshold of PTP induction. In the

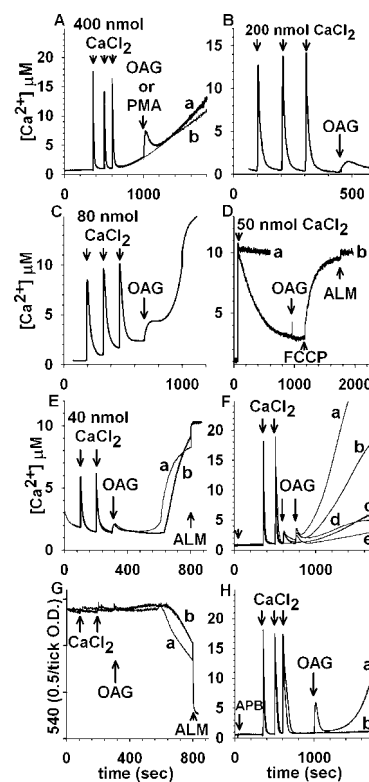


Fig. 1. OAG induces mitochondrial Ca²⁺ efflux and its relation to the permeability transition. Release of sequestered Ca²⁺ from rat brain (A, trace *a*), mouse kidney (B), mouse heart (C), and rat liver (E), but not sweet potato (D) mitochondria by the diacylglycerol analogue, OAG (100 μ M). The phorbol ester PMA (1 μ M) fails to induce Ca²⁺ release (A, trace *b*). In (D) trace *a*, Ru360 (165 nM) was present before addition of CaCl₂; in trace *b*, 1 μ M FCCP was added at 1200 s. (E): Rat liver mitochondria are loaded with two pulses of CaCl₂ (100 and 200 s, 40 nmol each) in the absence (trace *a*) or presence of Cys A (1 μ M, trace *b*), followed by addition of 100 μ M OAG at 300 s. At approximately 600 s, mitochondria spontaneously release Ca²⁺. Alamethicin (40 μ g/ml) was added at 800 s. (F): PTP inhibitors do not affect the initial OAG-induced Ca²⁺ efflux, but modulate the secondary rise: Rat brain mitochondria were loaded with two pulses of CaCl₂ (350 and 500 s, 400 nmol each) followed by addition of OAG (50 μ M) in the presence and absence of Cys A (2 μ M) or BKA (20 μ M) or 2-APB (100 μ M) (each added at 50 s, small arrow). In trace *a*, mitochondria were not pretreated with either PTP inhibitor; trace *b*, Cys A is present; trace *c*, mitochondria were not challenged by OAG (replaced with vehicle); trace *d*, mitochondria were pretreated with 2-APB; trace *e*, mitochondria were pretreated with BKA. (G): OAG does not evoke an immediate large-amplitude swelling in Ca²⁺-loaded rat liver mitochondria: Mitochondria were loaded with Ca²⁺ exactly as in (A) in the absence (trace *a*) or presence of Cys A (1 μ M, trace *b*), followed by addition of 100 μ M OAG at 300 s, and light scatter was followed spectrophotometrically. At approximately 600 s, mitochondria spontaneously swell. Alamethicin (40 μ g/ml) was added at 800 s. (H): 2-APB does not inhibit the initial OAG-induced Ca²⁺ release. Rat brain mitochondria were loaded with three pulses of CaCl₂ (350, 500, and 600 s, 400 nmol each) followed by addition of OAG at 1000 s in the presence of 2-APB (100 μ M, added at 50 s). Trace *a*, OAG (100 μ M) was added at 1000 s; in trace *b*, no OAG was added (replaced by vehicle). Traces for this and all subsequent figures are representative of at least four independent experiments unless otherwise indicated.

absence of OAG, Cys A elevated the threshold for PTP induction by CaCl₂ in rat liver mitochondria from 160 nmol/mg protein to 1280 nmol/mg protein. PTP inhibitors didn't affect the first or the second pulse of OAG-induced Ca²⁺ efflux (Fig. 1(F)); however, Cys A partially inhibited the secondary Ca²⁺ rise, while BKA and 2-APB conferred substantial protection (Fig. 1(F) and (H)).

OAG-Induced Ca²⁺ Release Is Not Mediated by the Uniporter or the Mitochondrial Na⁺/Ca²⁺ Exchanger

Inhibition of the uniporter by Ru360 fails to inhibit OAG-induced mitochondrial Ca²⁺ release and actually potentiates it (Fig. 2(A), trace *d*). Inhibition of the Na⁺/Ca²⁺ exchanger by CGP-37157 had no effect on modulating the OAG-induced Ca²⁺ release mechanism (Fig. 2(A), trace *e*). Addition of FCCP (Fig. 2(A), trace *c*), or antimycin A₃ plus oligomycin (trace *b*) in Ca²⁺-loaded mitochondria pretreated with Ru360 caused only a minor increase in the rate of Ca²⁺ efflux. La³⁺ abolishes OAG-induced Ca²⁺ release completely, but only moderately affects the reversal of the uniporter (Fig. 2(B)). Fura 6F reacts to La³⁺ similar to Ca²⁺, however the *K_d* of the dye for the trivalent is different (not quantified). Its presence also alters the *K_d* for Ca²⁺; therefore only qualitative measures of Ca²⁺ flux are possible after the addition of LaCl₃. La³⁺ is sequestered very slowly by mitochondria, competing with Ca²⁺ (Reed and Bygrave, 1974) and blocking the uniporter (Gunter and Pfeiffer, 1990). In trace *a*, addition of antimycin A₃ plus oligomycin induced slow Ca²⁺ efflux followed by faster release upon subsequent addition of FCCP. In trace *b* where no mitochondrial inhibitors were added, OAG-induced Ca²⁺ release was inhibited by LaCl₃. To address the directionality of the OAG-induced Ca²⁺ flux, mitochondria were not preloaded with CaCl₂, and Ru360 was added to eliminate Ca²⁺ uptake through the uniporter (Fig. 2(C), trace *a*). After subsequent addition of CaCl₂, there was no mitochondrial Ca²⁺ uptake and subsequent addition of OAG (trace *a*) had no effect on Fura 6F fluorescence. In contrast, Ca²⁺-loaded mitochondria subsequently exposed to Ru360 still exhibited OAG-induced Ca²⁺ efflux (trace *b*).

Effect of OAG on Mitochondrial Sr²⁺ Handling

Rat brain mitochondria were loaded with SrCl₂ (Fig. 3(A)) and flux of Sr²⁺ was monitored with Fura 6F. This dye responds to Sr²⁺ similarly to Ca²⁺; how-

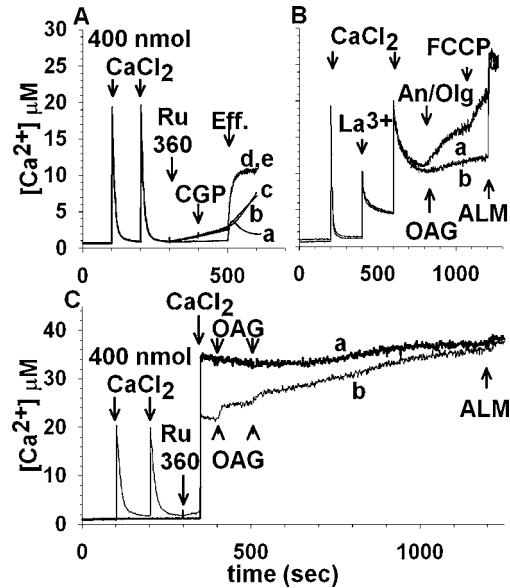


Fig. 2. OAG-induced Ca²⁺ efflux from rat brain mitochondria is not mediated by known Ca²⁺ uptake and release pathways. (A): Mitochondria are loaded by exogenously added Ca²⁺ (each pulse is 400 nmol CaCl₂) and the following compounds are administered: trace *a*, OAG (100 μM) at 500 s; trace *b*, 165 nM Ru360 at 300 s, 1 μM antimycin A₃ plus 2 μM oligomycin at 500 s; trace *c*, 165 nM Ru360 at 300 s, 0.5 μM FCCP at 500 s; trace *d*, 165 nM Ru360 at 300 s, 100 μM OAG at 500 s; trace *e*, 165 nM Ru360 at 300 s, 20 μM CGP-37157 at 400 s, 100 μM OAG at 500 s; traces *d* and *e* are superimposed. "Eff.": effectors. (B): 1 mM LaCl₃ abolishes OAG-induced Ca²⁺ efflux, without affecting the reverse function of the uniporter: mitochondria are treated with 400 nmol CaCl₂ at 350 and 600 s and 1 mM LaCl₃ in between (500 s). Subsequently 1 μM antimycin A₃ plus 2 μM oligomycin are administered at 800 s (trace *a*) or 100 μM OAG at 800 s (trace *b*). In trace *a* 0.5 μM FCCP was also added at 1100 s. In both traces, alamethicin (40 μg/ml) is added at 1200 s. (C): In trace *a*, rat brain mitochondria are not preloaded with Ca²⁺, and Ru360 (165 nM) is added at 300 s; subsequently, 800 nmol of CaCl₂ is added at 350 s, followed by two pulses of OAG (100 μM each) at 400 and 500 s. In trace *b*, mitochondria are preloaded with two pulses of exogenously added CaCl₂ (100 and 200 s, 400 nmol each); 165 nM Ru360 is added at 300 s, followed by an additional pulse of 400 nmol CaCl₂ at 350 s. Subsequently OAG (two pulses of 100 μM each) are added at 400 and 500 s. In both traces, alamethicin (40 μg/ml) is added at 1200 s.

ever, the *K_d* for Sr²⁺ is different (not quantified). In the absence of added OAG (trace *a*) mitochondria retain their Sr²⁺ load for the duration of the experiment. Addition of OAG (trace *b*) leads to an abrupt elevation of Fura 6F fluorescence, indicating release of sequestered Sr²⁺. The increase in Fura 6F fluorescence is not due to efflux of endogenous mitochondrial Ca²⁺ as addition of OAG (or FCCP, not shown) to freshly isolated mitochondria that have not been loaded with Ca²⁺ does not lead to an increase in Fura 6F fluorescence (Fig. 4(D)). Similar to the effect of La³⁺ on Ca²⁺ efflux, La³⁺ completely blocked OAG-induced Sr²⁺ release (Fig. 3(B)).

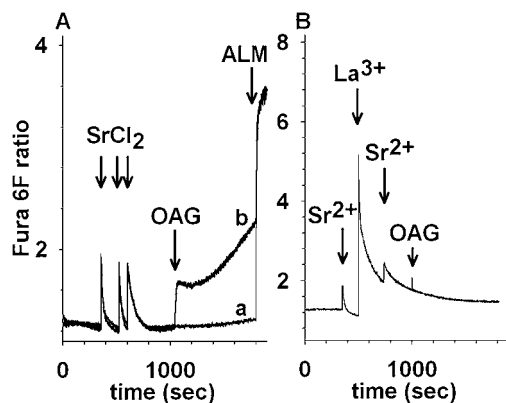


Fig. 3. OAG-induced Sr^{2+} efflux from rat brain mitochondria and inhibition by La^{3+} . (A): Mitochondria are loaded with three pulses of SrCl_2 (400 nmol each, trace *a*). In trace *b*, subsequent to Sr^{2+} loading, OAG is added (100 μM) at 1000 s causing an immediate increase in Fura 6F ratio fluorescence. In both traces, alamethicin (40 $\mu\text{g}/\text{ml}$) is added at 1800 s. (B): Mitochondria are treated with 400 nmol SrCl_2 at 350 and 750 s and 1 mM LaCl_3 in between (500 s). OAG is added (100 μM) at 1000 s causing no further increase in Fura 6F ratio fluorescence.

OAG Induces Cationic Channel Activity in Rat Brain Mitoplasts

In the absence of OAG, no channel activity was recorded from mitoplasts in 9 patches and conductances characteristic of PTP were observed in 3 other patches. Seventeen out of 34 patches showed no channel activity of any kind in the presence of OAG. Multiple conductance levels were observed in patches that were slightly cation-selective in the presence of OAG in 12 of 34 patches. These patches were scored positive for the presence of OAG-induced activity in the bar graph (Fig. 4(A), $p < 0.05$). While other transition sizes were observed, current traces recorded in the presence of OAG typically exhibited transitions of 202 ± 33 pS; ($n = 8$ patches, Fig. 4(B)–(D)). PTP and Tim23 channels with conductances of ~ 1200 and 750 pS, respectively, were recorded from 5 patches, which may have obscured the smaller OAG-induced activity (not shown). While the frequency of observing the OAG-induced activity increased slightly to 8 of 17 patches in the presence of the PTP inhibitor BKA, this increase was not statistically significant ($p = 0.4$). Unlike BKA, perfusing the excised patches that exhibited OAG-induced activity with 1 mM LaCl_3 led to a blockade of this channel activity ($n = 3$ patches). We did not observe any current upon exposure of OAG to patches excised from liposomes (Type IV, phosphatidylcholine, prepared as in (Guo *et al.*, 2004), Fig. 4(A)).

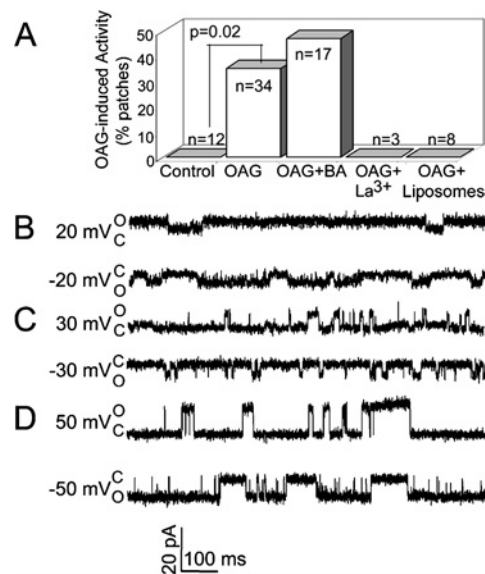


Fig. 4. OAG-induced mitoplast channel activity. (A): The frequency of detecting OAG-induced channel activity in rat brain mitoplasts is shown in the absence (Control) and presence (OAG) of 100 μM OAG, and presence of 100 μM OAG plus 20 μM BKA (OAG + BA). The frequency is statistically different in the absence and presence of OAG ($p = 0.02$) and is not statistically different in the presence and absence of BKA ($p = 0.4$, Fisher's test). The frequency of detecting OAG-induced activity in patches from giant liposomes is also shown (OAG + liposomes). "n" indicates the number of independent patches. (B–D). Current traces from three different excised patches from mitoplasts show 202 ± 33 pS (SD) transitions in the presence of 100 μM OAG at indicated voltages. O and C indicate open and closed current levels.

DAGs Release Mitochondrial Ca^{2+} Through a Mechanism Independent of DAG Metabolism or Activation of PKC

1,2-diacylglycerols other than OAG, release Ca^{2+} from Ca^{2+} -loaded mitochondria, (Fig. 5(A), traces *b–f*), while 1,3-diacylglycerols are inactive (Fig. 6(A)). Inhibition of PKC using five different PKC inhibitors (Fig. 5(B)) *potentiated* the OAG-induced initial Ca^{2+} efflux. No inhibitor exhibited statistically significant respiratory inhibition and/or uncoupling, except Myristoylated Protein Kinase C Inhibitor 20–28 (15% increase in state 4 respiration, not shown). The DAG lipase inhibitor RHC 80267 (Fig. 5(C), trace *b*) or the DAG kinase inhibitor II (Fig. 5(C), trace *c*) didn't influence significantly the initial OAG-induced Ca^{2+} efflux; RHC 80267 only slightly potentiated the initial OAG-induced Ca^{2+} efflux while the DAG kinase inhibitor II potentiated the delayed Ca^{2+} rise. Neither inhibitor exhibited respiratory inhibition or uncoupling (not shown). Addition of OAG to mitochondria prior to loading with CaCl_2 did not inhibit subsequent Ca^{2+} uptake; however, the time elapsed

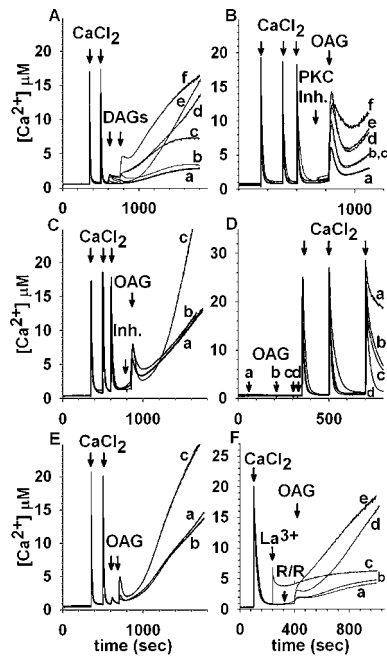


Fig. 5. Diacylglycerol-induced release of sequestered Ca²⁺ in rat brain mitochondria (A–E) and mitoplasts (F): Relationship to putative targets and catabolites. (A): Mitochondria are loaded with two pulses of CaCl₂ (400 nmol each at 350 and 500 s) followed by addition of the following DAG at 600 and 750 s (50 µM each pulse): trace *a*, vehicle (2 µl 96% ethanol [or DMSO, not shown]); trace *b*, DOL; trace *c*, DDC; trace *d*, SAG; trace *e*, DOG; trace *f*, HDAG. (B): PKC inhibitors potentiate the OAG-induced mitochondrial Ca²⁺ release: Mitochondria are loaded with three pulses of 400 nmol CaCl₂ (350, 500 and 600 s) and prior to addition of 100 µM OAG (850 s) the following PKC inhibitor is added at 800 s: trace *a*, vehicle (2 µl 96% ethanol); trace *b*, Ro-32-0432 (200 nM); trace *c*, Gö 6976 (100 nM); trace *d*, myristoylated PKC Inhibitor 20–28 (10 microM); trace *e*, chelerythrine chloride (1 microM) trace *f*, Bisindolylmaleimide I (30 nM). (C): Inhibition of OAG catabolism does not mitigate OAG-induced Ca²⁺ release: Mitochondria are loaded with three pulses of 400 nmol CaCl₂ (350, 500, and 600 s) and prior to addition of 100 µM OAG (850 s), inhibitors of DAG lipase and DAG lipase are added at 800 s. In trace *a*, no inhibitor is present, in trace *b* the DAG lipase inhibitor RHC 80267 (10 µM) is present; in trace *c*, the DAG kinase inhibitor “DAG kinase inhibitor II” (1 µM) was added at 800 s. (D): Addition of OAG to mitochondria that have not been loaded with Ca²⁺ does not abolish subsequent Ca²⁺ uptake. OAG (100 µM) was added at different time points at 50 s (trace *a*), 200 s (trace *b*), 300 s (trace *c*), 325 s (trace *d*), prior to challenging mitochondria with three pulses of CaCl₂ (at 350, 500, and 700 s, 400 nmol each). (E): Effect of phospholipids on the OAG-induced Ca²⁺ release: Mitochondria are loaded with two pulses of CaCl₂ (400 nmol each at 350 and 500 s) followed by addition of 25 µM OAG at 600 and 700 s in the presence of PS (10 µg/mg mitochondrial protein, trace *b*) or PE (10 µg/mg mitochondrial protein, trace *c*). In trace *a*, ethanol was added instead of a phospholipid. (F): OAG releases sequestered Ca²⁺ from rat brain mitoplasts: In all traces, mitoplasts are loaded with a single pulse of 400 nmol CaCl₂ (100 s), and OAG (100 µM unless otherwise indicated) is added at 400 s. In trace *a*, no further additions were made. In trace *b*, RHC 80267 (10 µM) was added at 320 s; in trace *c*, 1 mM LaCl₃ was added at 240 s; in trace *d*, 200 µM OAG was added at 400 s; in trace *e*, 165 nM Ru360 was added at 320 s, followed by 200 µM OAG at 400 s. “R/R” signifies RHC 80267 or Ru360.

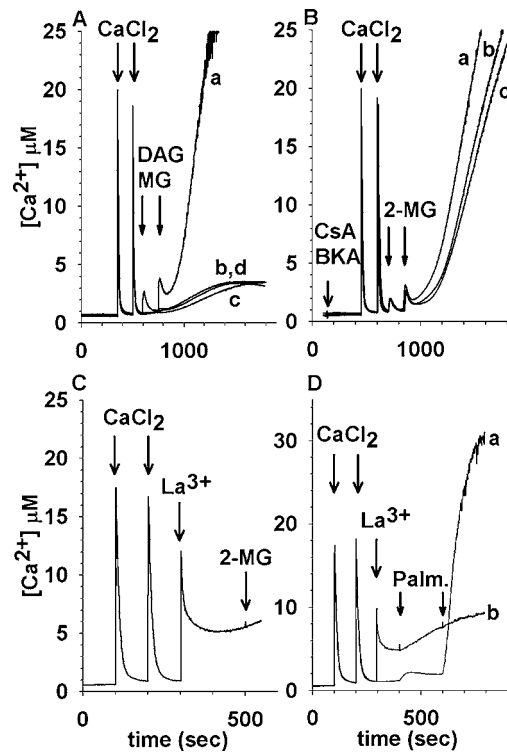


Fig. 6. Di- and Monoacylglycerol induced mitochondrial Ca²⁺ release: Effects of permeability transition inhibition and La³⁺. (A): Mitochondria are loaded with two pulses of CaCl₂ (400 nmol each at 350 and 500 s) followed by addition of the following DAG or MG at 600 and 750 s (100 µM each pulse): trace *a*, 2-Monooleoylglycerol (C18:1, [*cis*]-9); trace *b*, 1,3-Di-([*cis*]-9-octadecenoyl)-rac-glycerol; trace *c*, vehicle; trace *d*, 1-Monooleoyl-rac-glycerol (C18:1, [*cis*]-9). (B): Mitochondria are pretreated with a PTP inhibitor (at 50 s) and challenged with two pulses of CaCl₂ (400 nmol each at 350 and 500 s) followed by addition of 2-Monooleoylglycerol at 600 and 750 s (50 µM each pulse); trace *a*, no PTP inhibitor; trace *b*, 2 µM Cys A; trace *c*, 20 µM BKA. (C): LaCl₃ inhibits the 2-MG induced Ca²⁺ efflux: Mitochondria are loaded with two pulses of CaCl₂ (400 nmol each at 100 and 200 s) followed by addition of 1 mM LaCl₃ at 300 s; subsequently, 100 µM 2-Monooleoylglycerol is added at 500 s. (D): LaCl₃ inhibits the palmitic acid-induced Ca²⁺ efflux: In trace *a*, mitochondria are loaded with two pulses of CaCl₂ (400 nmol each at 100 and 200 s); subsequently, 10 µM palmitic acid is added at 400 and 600 s; in trace *b*, mitochondria are loaded with two pulses of CaCl₂ (400 nmol each at 100 and 200 s) followed by addition of 1 mM LaCl₃ at 300 s; subsequently, 10 µM palmitic acid is added at 400 and 600 s.

before the addition of OAG to the point of Ca²⁺ challenge influenced the maximal Ca²⁺ uptake capacity of mitochondria (Fig. 5(D), traces *a–d*). Various PLC inhibitors (U-73122, Edelfosine, D609, neomycin) were tested for their effects on maximal Ca²⁺ uptake capacity with the exception of neomycin with these drugs inhibited uptake due to the finding that they are potent respiratory uncouplers (not shown). Inclusion of phospholipids

(phosphatidylethanolamine [PE] vs. phosphatidylserine [PS]) in the medium enhanced the potency of the second pulse of OAG-induced Ca^{2+} efflux from Ca^{2+} -loaded mitochondria (Fig. 5(E)). Addition of OAG to mitoplasts caused release of sequestered Ca^{2+} (Fig. 5(F), trace *a*). The presence of RHC 80267 did not alter the initial OAG-induced Ca^{2+} efflux. The effect of OAG was further potentiated in the presence of Ru360 (Fig. 5(F), trace *e*). Pretreatment of Ca^{2+} -loaded mitoplasts with 1 mM LaCl_3 prior to addition of OAG blocked the effect of the diacylglycerol on releasing stored Ca^{2+} (Fig. 5(F), trace *c*).

Additional Characteristics of DAG-Induced Release of Mitochondrial Ca^{2+}

We compared the effect of OAG to 1,3-diolein (1,3-Di-([*cis*]-9-octadecenoyl)-rac-glycerol, (Fig. 6(A), trace *b*), 2-MG (2-Monooleoylglycerol (C18:1, [*cis*]-9) (trace *a*) and 1-MG (1-Monooleoyl-rac-glycerol (C18:1, [*cis*]-9), (trace *d*). Only 2-MG induced an initial Ca^{2+} efflux from Ca^{2+} -loaded rat brain mitochondria, followed by a robust delayed Ca^{2+} rise (Fig. 6(A), trace *a*). Neither the initial 2-MG-induced Ca^{2+} release nor the delayed Ca^{2+} efflux was sensitive to PTP inhibitors (Fig. 6(B), traces *b* and *c*). The 2-MG-induced Ca^{2+} release was, however, completely abolished by 1 mM LaCl_3 (Fig. 6(C)). 1 mM LaCl_3 also inhibited release of sequestered Ca^{2+} from rat brain mitochondria induced by palmitic acid (Fig. 6(D)). Moreover, LaCl_3 mitigated the uncoupling effect of this fatty acid (not shown). 2-MG exhibited both significant uncoupling and inhibition of state 3 respiration (Table I). Among the DAGs, DOG exhibited significant uncoupling.

The other tested DAGs, including OAG, exhibited little or no inhibition of state 3 respiration.

DISCUSSION

The novel observations of the current study point to a potential mode of Ca^{2+} release in mitochondria that can be synchronized with physiological events inducing elevation of cytosolic [Ca^{2+}] either throughout the cell or in microdomains. Our primary finding is that OAG releases Ca^{2+} sequestered by mitochondria isolated from rodent tissues but not from sweet potato. Plants do possess multiple pathways that ultimately result in DAGs production (Wang, 2004). The importance of the lack of effect of OAG on sweet potato mitochondria is twofold: (i) it demonstrates biological diversity and (ii) it weakens the possibility of an artifact of OAG on lipid membranes, implicated previously (Allan *et al.*, 1978; Leikin *et al.*, 1996; Szule *et al.*, 2002).

Additional lines of evidence argue against a Ca^{2+} -ionophoretic activity of the diacylglycerol or an unspecific effect on bilayers leading to ion permeability: (i) following Ca^{2+} release upon exposure to OAG in mammalian mitochondria, extramitochondrial [Ca^{2+}] returns to baseline values; an ionophore would lead to the establishment of a new steady-state [Ca^{2+}]; (ii) OAG does not cause any swelling during the initial Ca^{2+} release, excluding the possibility of an unspecific hole-forming effect or activation of the PTP; (iii) several effective 1,2-DAGs do not exhibit any uncoupling properties that would be obvious if they nonselectively permeabilize the mitochondrial inner membrane; (iv) application of OAG to the patches

Table I. Effects of Di- and Monoacylglycerols and Farnesyl Thiotriazole (FTT) on Rat Brain Mitochondrial Oxygen Consumption

	State 3	State 4 (effector added before oligomycin)	State 4 (effector added after oligomycin)
Vehicle, (<i>n</i> = 12)	131 ± 3	16 ± 1	16 ± 1
OAG (<i>n</i> = 6)	102 ± 4*	16 ± 1 ^{ns}	16 ± 1 ^{ns}
2-MG (<i>n</i> = 5)	110 ± 9*	29 ± 2*	15 ± 1 ^{ns}
DDC (<i>n</i> = 3)	125 ± 6 ^{ns}	15 ± 1 ^{ns}	14 ± 1 ^{ns}
DOL (<i>n</i> = 3)	113 ± 6*	15 ± 1 ^{ns}	14 ± 1 ^{ns}
DOG (<i>n</i> = 3)	130 ± 9 ^{ns}	21 ± 2*	17 ± 1 ^{ns}
FTT (<i>n</i> = 3)	48 ± 4*	34 ± 2*	29 ± 2*
HDAG (<i>n</i> = 3)	96 ± 5*	14 ± 1 ^{ns}	15 ± 1 ^{ns}
SAG (<i>n</i> = 3)	126 ± 7 ^{ns}	15 ± 1 ^{ns}	14 ± 1 ^{ns}

Note. All di- and monoacylglycerols and FTT were tested at 100 μM concentration. *n*: number of independent experiments. Statistics: Mann-Whitney rank sum test; *: significant compared to control (vehicle), *p* < 0.001, ns: not significant compared to control. Values are given as nmol/min/mg protein and expressed as standard errors of the mean, rounded to the nearest integer.

does not always result in channel activity, arguing against a nonspecific membrane stressing effect; (v) no currents are observed with patched liposomes upon exposure to the diacylglycerol.

To test the hypothesis that OAG induces Ca²⁺ efflux through previously described mitochondrial flux pathways, we blocked independently the uniporter, the Na⁺/Ca²⁺ exchanger, and the PTP. Blocking the uniporter with Ru360 preventing bidirectional Ca²⁺ transport by this pathway (Matlib *et al.*, 1998) does not inhibit and, as expected, actually potentiates the OAG-induced Ca²⁺ release from mitochondria or mitoplasts; the amplitude of the release is greater in the presence of Ru360 due to the inability of the uniporter to reaccumulate Ca²⁺, hence also the lack of post-OAG extramitochondrial [Ca²⁺] decay. This observation also argues against an uncoupling mode of action of OAG since uncoupler-induced calcium efflux occurs via reversal of the mitochondrial uniporter (Bernardi *et al.*, 1984). In addition, the uniporter is relatively impermeable to K⁺ while our electrophysiological recordings were made using symmetrical KCl solutions. Moreover, single uniporter channels have multiple sub-conductance states between 2.6 pS and 5.2 pS at -160 mV, but the OAG-induced conductances are ~200 pS. Therefore, it is clear that the OAG-induced channel is not the uniporter characterized recently (Kirichok *et al.*, 2004). La³⁺ inhibits completely the OAG response, while in our hands, La³⁺ (1 mM) does not eliminate the release of Ca²⁺ from mitochondria induced by respiratory inhibition or uncoupling. Blockade of the Na⁺/Ca²⁺ exchanger with CGP-37157 does not antagonize the OAG effect; moreover, the fast kinetics of the initial OAG-induced Ca²⁺ efflux argue against the involvement of a slow exchanger. In addition, the absence of Na⁺ in the medium eliminates the Na⁺/Ca²⁺ exchanger as the mechanism.

We furthermore conclude that the initial rapid Ca²⁺ efflux induced by OAG is not due to PTP opening because: (i) it is insensitive to any PTP inhibitor tested; (ii) OAG-induced channel activity exhibits conductances ~6 times lower than those characteristics of PTP (Loupatatzis *et al.*, 2002); (iii) OAG induces Sr²⁺ release from Sr²⁺-loaded mitochondria, whereas Sr²⁺ does not promote PTP formation (Hunter *et al.*, 1976); (iv) OAG does not induce any large-amplitude swelling during the initial Ca²⁺ release and, in accordance with our observations, DAGs were shown earlier not to induce swelling of liver mitochondria (Pastorino *et al.*, 1999). In contrast, the delayed Ca²⁺ rise exhibits robust evidence of PTP, including sensitivity to PTP inhibitors and large-amplitude mitochondrial swelling. At least one component leading to the delayed formation of PTP is the intense Ca²⁺ cycling substantiated by the OAG-induced Ca²⁺ channel(s) and the uniporter;

however, in rat liver mitochondria, the presence of Cys A did not extend significantly the threshold for PTP induction in the presence of OAG, in spite of the immensely protecting effect of the immunophilin against high-Ca²⁺ mitochondrial loading in the absence of the diacylglycerol. Since DAGs activate PLA₂ which is also found in mitochondria (Nachbaur and Vignais, 1968), the OAG induced secondary phase of Ca²⁺ release could be due to activation of this enzyme, which is known to contribute to induction and/or maintenance of PTP (Broekemeier and Pfeiffer, 1989; Rustenbeck *et al.*, 1996); however, neither aristolochic acid, nor bromoenol lactone (both inhibitors of PLA₂) inhibited mitochondrial Ca²⁺-induced Ca²⁺ release (mCICR) under the exact conditions in the absence of OAG (Chinopoulos *et al.*, 2003).

Phorbol esters can substitute for diacylglycerol in activating both protein kinase C (Nishizuka, 1995) and non-PKC (Brose *et al.*, 2004). Substitution of OAG for PMA fails to induce Ca²⁺ efflux. Moreover, inclusion of five different PKC inhibitors does not ameliorate the OAG effect and even potentiates it. Such a scenario has been reported for DAG-sensitive TRP channels on the plasma membrane (Venkatachalam *et al.*, 2003). However, the possibility of TRP channels being present in mitochondria has been previously excluded (Chinopoulos *et al.*, 2003). A caveat here is that contemporary pharmacological PKC antagonists targeting the C1 domain bind with similar affinities to non-PKCs possessing the same domain activated by DAG/phorbol esters (Yang and Kazanietz, 2003). The question arises, as to why would there be PKC in our isolated mitochondria preparations, since it translocates to the organelles as a reaction to cell stress; probably, the mitochondrial isolation procedure is damaging enough (decapitation of the animal, transient hypoxia of the tissue) to cause PKC translocation.

To characterize further the mode of action of DAGs on mitochondria, we tested di- and monoacylglycerols by varying the position of the acyl groups. Only 1,2-sn-DAGs induce release of Ca²⁺, while 1,3-sn-DAGs are inactive. Among monoacylglycerols, 1-MG is not effective, as opposed to 2-MG that releases Ca²⁺ vigorously. As a comparison, PKC is not activated by 1,3-DAGs nor monoacylglycerols, but is activated by 1,2-DAGs (Nishizuka, 1995). 2-MG induces powerful uncoupling in addition to causing Ca²⁺ efflux that is insensitive to PTP inhibitors. At this juncture, it is not known if 2-MGs and 1,2-DAGs share the same target(s) on mitochondria or if 2-MG has an alternative mode of action. La³⁺ inhibits the 2-MG-induced Ca²⁺ release completely; however, La³⁺ also inhibits palmitic acid-induced PTP (Sultan and Sokolove, 2001) and Ca²⁺ flux through the uniporter. The universal ability of La³⁺ to block all forms of mitochondrial Ca²⁺

release therefore limits its usefulness in delineating the individual mechanism involved in OAG-induced release.

In addition to regulation by diacylglycerol or phorbol esters, DAG targets require Ca^{2+} and PS (Bell and Burns, 1991). Inclusion of PS to the suspension does not have an effect on the OAG-induced Ca^{2+} efflux; however, PE potentiates the OAG response. At this juncture, we cannot attribute the PE potentiating effect on a biologically relevant mechanism or on the possibility that PE is a better vehicle for OAG in solution. Concerning the requirement of matrix Ca^{2+} , our experiments demonstrate that OAG causes release of Ca^{2+} from Ca^{2+} -loaded mitochondria but does not allow Ca^{2+} influx in mitochondria treated with Ru360. It is therefore possible that the target molecule(s) of OAG on the inner mitochondrial membrane possess binding site(s) for Ca^{2+} located at the inner leaflet of the membrane. This is a very similar scenario to the one involving PKC: Ca^{2+} increases the affinity of conventional PKCs for negatively charged lipids and this increase varies linearly with Ca^{2+} concentration in the low μM to submillimolar range (Mosior and Epan, 1994). OAG also releases sequestered strontium; however, due to the almost identical molecular radius of Sr^{2+} to Ca^{2+} , Sr^{2+} may substitute for Ca^{2+} for whatever means. The requirement for accumulated intramitochondrial Ca^{2+} for DAGs-induced Ca^{2+} release can be envisioned as a mechanism preventing mitochondria from buffering all the Ca^{2+} coming from other sources during PIP_2 hydrolysis. The necessity of an obligatory metabolite (DAG) sets the mechanism in synchrony.

It is clear that mitochondria host DAG targets (see Introduction), though the two major DAG clearance pathways, DAG kinase and DAG lipase, have not been unequivocally identified these organelles (Bothmer *et al.*, 1992); nevertheless, 1,2-diacyl-sn-glycerol is a reactant or product in 23 reactions, spanning among four different biochemical pathways (for a complete description of the involvement of DAGs in biochemical pathways, see: http://www.genome.jp/dbget-bin/www_bget?compound±C00641), leaving multiple candidates for DAG clearance; parts from the overall reactions in all four pathways are hosted by mitochondrial membranes or take place in the matrix (Murray, 2003).

In summary, DAGs release sequestered Ca^{2+} from isolated mitochondria, most likely mediated through novel channels located on the inner mitochondrial membrane, or a single channel with multiple substates. It remains to be determined if DAGs are the physiological inducers for this channel activity during signal transduction in cells associated with activation of phospholipase C. This is an exciting possibility linking the triad of signal transduction, intracellular Ca^{2+} homeostasis, and mitochondrial bioenergetics.

ACKNOWLEDGMENTS

We thank Dr. Alicia J. Kowaltowski for help with the sweet potato mitochondrial isolation and Prof. Miklós Tóth and Dr. György Báthori for comments during the preparation of the manuscript. This work was supported by NIH grant GM57249 and NSF grant MCB-0235834 to K.W.K. and NIH grant NS34152 and USAMRMC grant DAMD 17-99-1-9483 to G.F.

REFERENCES

- Allan, D., Thomas, P., and Michell, R. H. (1978). *Nature* **276**, 289–290.
- Baines, C. P., Song, C. X., Zheng, Y. T., Wang, G. W., Zhang, J., Wang, O. L., Guo, Y., Bolli, R., Cardwell, E. M., and Ping, P. (2003). *Circ. Res.* **92**, 873–880.
- Bell, R. M., and Burns, D. J. (1991). *J. Biol. Chem.* **266**, 4661–4664.
- Bernardi, P., Paradisi, V., Pozzan, T., and Azzone, G. F. (1984). *Biochemistry* **23**, 1645–1651.
- Bernardi, P., Vassanelli, S., Veronese, P., Colonna, R., Szabo, I., and Zoratti, M. (1992). *J. Biol. Chem.* **267**, 2934–2939.
- Bothmer, J., Markerink, M., and Jolles, J. (1992). *Biochem. Biophys. Res. Commun.* **187**, 1077–1082.
- Broekemeier, K. M., and Pfeiffer, D. R. (1989). *Biochem. Biophys. Res. Commun.* **163**, 561–566.
- Brose, N., Betz, A., and Wegmeyer, H. (2004). *Curr. Opin. Neurobiol.* **14**, 328–340.
- Brose, N., and Rosenmund, C. (2002). *J. Cell Sci.* **115**, 4399–4411.
- Chen, C. H., and Lehninger, A. L. (1973). *Arch. Biochem. Biophys.* **157**, 183–196.
- Chinopoulos, C., Starkov, A. A., and Fiskum, G. (2003). *J. Biol. Chem.* **278**, 27382–27389.
- Clapham, D. E. (2003). *Nature* **426**, 517–524.
- Clapham, D. E., Montell, C., Schultz, G., and Julius, D. (2003). *Pharmacol. Rev.* **55**, 591–596.
- Florin-Christensen, J., Florin-Christensen, M., Delfino, J. M., Stegmann, T., and Rasmussen, H. (1992). *J. Biol. Chem.* **267**, 14783–14789.
- Ford, D. A., and Gross, R. W. (1990). *J. Biol. Chem.* **265**, 12280–12286.
- Freeman, M., and Mangiapane, E. H. (1989). *Biochem. J.* **263**, 589–595.
- Gudermann, T., Hofmann, T., Schnitzler, M., and Dietrich, A. (2004). *Novartis Found. Symp.* **258**, 103–118.
- Gunter, T. E., and Pfeiffer, D. R. (1990). *Am. J. Physiol.* **258**, C755–C786.
- Guo, L., Pietkiewicz, D., Pavlov, E. V., Grigoriev, S. M., Kasianowicz, J. J., Dejean, L. M., Korsmeyer, S. J., Antonsson, B., and Kinnally, K. W. (2004). *Am. J. Physiol. Cell Physiol.* **286**, C1109–C1117.
- Hofmann, T., Obukhov, A. G., Schaefer, M., Harteneck, C., Gudermann, T., and Schultz, G. (1999). *Nature* **397**, 259–263.
- Hunter, D. R., Haworth, R. A., and Southard, J. H. (1976). *J. Biol. Chem.* **251**, 5069–5077.
- Irvine, R. F. (2002). *Sci. STKE* 2002, RE13.
- Kazanietz, M. G. (2002). *Mol. Pharmacol.* **61**, 759–767.
- Kirichok, Y., Krapivinsky, G., and Clapham, D. E. (2004). *Nature* **427**, 360–364.
- Knox, C. D., Belous, A. E., Pierce, J. M., Wakata, A., Nicoud, I. B., Anderson, C. D., Pinson, C. W., and Chari, R. S. (2004). *Am. J. Physiol. Gastrointest. Liver Physiol.* **287**, G533–G540.
- Korge, P., Honda, H. M., and Weiss, J. N. (2002). *Proc. Natl. Acad. Sci. U.S.A.* **99**, 3312–3317.
- Lee, C., Fisher, S. K., Agranoff, B. W., and Hajra, A. K. (1991). *J. Biol. Chem.* **266**, 22837–22846.
- Leikin, S., Kozlov, M. M., Fuller, N. L., and Rand, R. P. (1996). *Biophys. J.* **71**, 2623–2632.

- Li, L., Lorenzo, P. S., Bogi, K., Blumberg, P. M., and Yuspa, S. H. (1999). *Mol. Cell Biol.* **19**, 8547–8558.
- Liscovitch, M., Czarny, M., Fiucci, G., Lavie, Y., and Tang, X. (1999). *Biochim. Biophys. Acta* **1439**, 245–263.
- Loupatatzis, C., Seitz, G., Schonfeld, P., Lang, F., and Siemen, D. (2002). *Cell. Physiol. Biochem.* **12**, 269–278.
- Majumder, P. K., Pandey, P., Sun, X., Cheng, K., Datta, R., Saxena, S., Kharbanda, S., and Kufe, D. (2000). *J. Biol. Chem.* **275**, 21793–21796.
- Matlib, M. A., Zhou, Z., Knight, S., Ahmed, S., Choi, K. M., Krause-Bauer, J., Phillips, R., Altschuld, R., Katsube, Y., Sperelakis, N., and Bers, D. M. (1998). *J. Biol. Chem.* **273**, 10223–10231.
- Mikoshiha, K., and Hattori, M. (2000). *Sci. STKE* 2000, E1.
- Mosior, M., and Epan, R. M. (1994). *J. Biol. Chem.* **269**, 13798–13805.
- Murray, R. K. (2003). *Harper's Illustrated Biochemistry*, Lange Medical Books/McGraw-Hill, New York.
- Murriel, C. L., Churchill, E., Inagaki, K., Szweda, L. I., and Mochly-Rosen, D. (2004). *J. Biol. Chem.* **279**, 47985–47991.
- Nachbaur, J., and Vignais, P. M. (1968). *Biochem. Biophys. Res. Commun.* **33**, 315–320.
- Nilius, B. (2004). *Sci. STKE* 2004, e36.
- Nishihira, J., and Ishibashi, T. (1986). *Lipids* **21**, 780–785.
- Nishizuka, Y. (1992). *Science* **258**, 607–614.
- Nishizuka, Y. (1995). *FASEB J.* **9**, 484–496.
- Okada, T., Inoue, R., Yamazaki, K., Maeda, A., Kurosaki, T., Yamakuni, T., Tanaka, I., Shimizu, S., Ikenaka, K., Imoto, K., and Mori, Y. (1999). *J. Biol. Chem.* **274**, 27359–27370.
- Panagia, V., Ou, C., Taira, Y., Dai, J., and Dhalla, N. S. (1991). *Biochim. Biophys. Acta* **1064**, 242–250.
- Pastorino, J. G., Tafani, M., Rothman, R. J., Marcinkeviciute, A., Hoek, J. B., Farber, J. L., and Marcineviciute, A. (1999). *J. Biol. Chem.* **274**, 31734–31739.
- Penner, R., and Fleig, A. (2004). *Sci. STKE* 2004, e38.
- Putney, J. W. Jr. (1986). *Cell Calcium* **7**, 1–12.
- Rajdev, S., and Reynolds, I. J. (1993). *Neurosci. Lett.* **162**, 149–152.
- Rebecchi, M. J., and Pentylala, S. N. (2000). *Physiol. Rev.* **80**, 1291–1335.
- Reed, K. C., and Bygrave, F. L. (1974). *Biochem. J.* **140**, 143–155.
- Rustenbeck, I., Munster, W., and Lenzen, S. (1996). *Biochim. Biophys. Acta* **1304**, 129–138.
- Ruvolo, P. P., Deng, X., Carr, B. K., and May, W. S. (1998). *J. Biol. Chem.* **273**, 25436–25442.
- Sato, T., O'Rourke, B., and Marban, E. (1998). *Circ. Res.* **83**, 110–114.
- Schmidt, B., Wachter, E., Sebal, W., and Neupert, W. (1984). *Eur. J. Biochem.* **144**, 581–588.
- Schnaitman, C., Erwin, V. G., and Greenawalt, J. W. (1967). *J. Cell Biol.* **32**, 719–735.
- Starkov, A. A., and Fiskum, G. (2001). *Biochem. Biophys. Res. Commun.* **281**, 645–650.
- Storz, P., Hausser, A., Link, G., Dedio, J., Ghebrehiwet, B., Pfizenmaier, K., and Johannes, F. J. (2000). *J. Biol. Chem.* **275**, 24601–24607.
- Sultan, A., and Sokolove, P. M. (2001). *Arch. Biochem. Biophys.* **386**, 52–61.
- Szule, J. A., Fuller, N. L., and Rand, R. P. (2002). *Biophys. J.* **83**, 977–984.
- Vaena de, A. S., Okamoto, Y., and Hannun, Y. A. (2004). *J. Biol. Chem.* **279**, 11537–11545.
- Venkatachalam, K., van Rossum, D. B., Patterson, R. L., Ma, H. T., and Gill, D. L. (2002). *Nat. Cell Biol.* **4**, E263–E272.
- Venkatachalam, K., Zheng, F., and Gill, D. L. (2003). *J. Biol. Chem.* **278**, 29031–29040.
- Wang, X. (2004). *Curr. Opin. Plant Biol.* **7**, 329–336.
- Watt, S. A., Kular, G., Fleming, I. N., Downes, C. P., and Lucocq, J. M. (2002). *Biochem. J.* **363**, 657–666.
- Yang, C., and Kazanietz, M. G. (2003). *Trends Pharmacol. Sci.* **24**, 602–608.